

Performance Bounds for Cooperative Localisation in Starlink

Turner, C.J.; Rajan, R.T.

Publication date

2022

Document Version

Accepted author manuscript

Published in

73rd International Astronautical Congress (IAC)

Citation (APA)

Turner, C. J., & Rajan, R. T. (2022). Performance Bounds for Cooperative Localisation in Starlink. In *73rd International Astronautical Congress (IAC)* <https://iafastro.directory/iac/proceedings/IAC-22/IAC-22/B2/IPB/manuscripts/IAC-22,B2,IPB,3,x73516.pdf>

Important note

To cite this publication, please use the final published version (if applicable). Please check the document version above.

Copyright

Other than for strictly personal use, it is not permitted to download, forward or distribute the text or part of it, without the consent of the author(s) and/or copyright holder(s), unless the work is under an open content license such as Creative Commons.

Takedown policy

Please contact us and provide details if you believe this document breaches copyrights. We will remove access to the work immediately and investigate your claim.

Performance Bounds for Cooperative Localisation in Starlink Calum Turner^{ab}, Raj Thilak Rajan^{b*}

^a ISAE-SUPAERO, Toulouse, France

^b Technical University of Delft, The Netherlands, r.t.rajan@tudelft.nl

* Corresponding Author

Abstract

Large satellite constellations in Low Earth Orbit (LEO) have the potential to revolutionise worldwide internet access. The concomitant potential of these large constellations to impact space sustainability, however, has prompted concern from space actors as well as provoking concern in the ground-based astronomy community. Increasing the positional accuracy of the orbital state of satellites in mega-constellations improves space situational awareness, reducing the need for collision avoidance manoeuvres and allowing astronomers to prepare better observational mitigation strategies. Current state-of-the-art solutions rely on Earth-based ground segments or onboard Global Navigation Satellite Systems hardware to precisely localise satellites. These methods can be augmented by cooperative navigation within the satellite network using existing intersatellite links. In this paper, we present a model of Phase 1 of Starlink, one of the more well-studied large constellations in LEO and investigate the potential of cooperative localisation using time-of-arrival measurements from the optical intersatellite links in the constellation. We establish the achievable performance of cooperative localisation between 1584 Starlink satellites and 87 ground stations by calculating the theoretical lower bounds on the accuracy of the position estimation e.g., Cramér-Rao Bound over the course of one orbit at 573 simulated time steps. Our results show that the standard deviation for localising the Starlink satellites has a value of 10.15 m and varies between a maximum of 36.5 m and a minimum of approximately 2m. This result is determined primarily by the geometry of the constellation and the characteristics of the intersatellite links. We discuss our results and lay out options for more sophisticated modelling and investigations for improved position accuracy of large satellite constellations.

Keywords: (Starlink, Cooperative Navigation, Space Situational Awareness, Megaconstellation)

Nomenclature

R_E	Earth Radius
d	Maximum satellite-to-ground-station distance
a	Altitude
ϵ_0	Elevation of a satellite above a ground station horizon
n	Number of satellites with unknown locations
m	Number of ground stations with known locations
$H(i)$	Set of nodes satellite i can communicate with
d_{ij}	Distance between satellite i and node j
γ	Measurement-dependent channel constant
\mathbf{F}	Fisher Information Matrix
x_i, y_i, z_i	Position of node i

Acronyms

CRB	Cramér-Rao Bound
FCC	Federal Communications Commission
FIM	Fisher Information Matrix
LEO	Low Earth Orbit
LOS	Line of Sight
RCRB	Root Cramér-Rao Bound
ToA	Time of Arrival

1. Introduction

Space traffic management and space situational awareness are both aided by improved knowledge of the orbital state of satellites. Satellites' positions and orbital elements are determined either by onboard hardware or through tracking via ground stations. In addition to these methods, intersatellite links could allow cooperative localisation to be performed based on satellite-to-satellite measurements. This provides additional information to operators seeking to improve space situational awareness, reduces dependency on ground stations, and provides a redundant method of localising satellites to any guidance and navigation hardware on board. The improved knowledge of orbital position can benefit space sustainability beyond space traffic management. Knowing the precise location of satellites allows astronomers to time their observations to avoid satellite trails, which would otherwise saturate the sensitive detectors in large telescopes. [1]

Using intersatellite measurements for cooperative navigation has received growing academic attention in the last several years, with research investigating the performance of autonomous navigation using laser intersatellite links in a variety of Earth orbits [2] and investigating the use of laser intersatellite links for precise orbit determination in constellations of up to 192

satellites [3]. However, to our knowledge cooperative localisation has not yet been studied for mega constellations of thousands of satellites. In this paper, we explored the potential of cooperative localisation using time-of-arrival measurements from the optical intersatellite links in Phase 1 of Starlink. While many mega constellations have been proposed or are being constructed, we choose to model Starlink because it is a relatively well-studied Low Earth Orbit (LEO) constellation that will employ optical intersatellite links. Starlink is a network of thousands of satellites which will exchange and transmit data to provide low-latency internet worldwide [4]. Starlink is also an interesting case study as it has been noted as contributing to concerns about space sustainability [5] and interference with ground-based astronomy [6,7]. Previous research has also addressed the intersatellite links between Starlink satellites and the resulting network topology [8,9], which also influenced our choice of Starlink as a case study.

This paper is organised as follows. First, in Section 2.1, we create a spatial model of Phase 1 of the Starlink network, which represents the locations of the satellites over the course of one orbit. We establish the location of Starlink ground stations in Section 2.2 and explore the network topology of the system in Sections 2.3 and 2.4. We then calculate the Cramér-Rao Bound (CRB) using the equations in Section 3 and present our results in Section 4. We conclude the paper with a discussion of our results and a summary of ongoing and future work.

2. Methods

In this section we describe our model of Phase 1 of Starlink, the assumed network topology of the system, and the location of ground stations.

2.1 Creating the Starlink Network

To provide reference positions for simulations of cooperative localisation, a model of Starlink was created using Python. The model consisted of 1584 satellites in Low Earth Orbit at an altitude of 550 km, corresponding to Phase 1 of the Starlink constellation. The satellites are split equally into 72 planes each at an inclination of $i=53^\circ$. The details of this constellation design were based on the information in an FCC filing dated April 17, 2020 [10] and are shown in Table 1.

Table 1. Model Parameters for Phase 1 of Starlink

Altitude	550 km
Number of Planes	72
Satellites per Plane	22
Inclination	53°
Orbital Period T	1.59 hours

This dataset was published on IEEE DataPort™ as an open-access dataset [11], and the code was made available on GitHub [12]. The orbits—which were assumed to be circular—were propagated using a built-in Polastro [13] function which provided the position and velocity of each satellite in Cartesian coordinates. The J2 effect was calculated for each satellite but aerodynamic drag was found to have a negligible effect on the satellite positions over the course of one orbit and was therefore omitted. Following the methodology in [8], each Starlink satellite was given a unique identifier with the format $sXXYYY$ where XX is plane number and YYY is the satellite number in base 10. For example, the first satellite in the first plane has the identifier $s01001$ and has initial position $[a, 0, 0]$ where a is the semi-major axis of the orbit.

2.2 Locating the Ground Stations

To calculate the performance bounds on cooperative localisation satellites in the Starlink network also requires the location of the constellation’s ground stations to be known. This allows the satellites visible from any given ground stations at any given time to be calculated. Figure 1 shows the location of 87 planned or active Starlink ground stations as based on regulatory filings in the USA, Chile, UK, France, Australia, and New Zealand. We calculated the maximum distance between ground stations and satellites under the constraint of line-of-sight visibility using the equations detailed in [14]. The geometric set-up for this calculation is shown in Figure 2, and the expression for finding the maximum distance is:

$$d = R_E \left[\sqrt{\left(\frac{a + R_E}{R_E}\right)^2 - 1} \right] \quad (1)$$

Where the nomenclature is shown at the beginning of this paper. The value ϵ_0 in Figure 2 is the elevation of the satellite above the ground station’s local horizon; when considering if a Starlink satellite was in range of a ground station in our simulations we chose a relatively conservative value of $\epsilon_0 = 40^\circ$ to account for Line Of Sight (LOS) barriers such as hills, forests, or buildings.

2.3 Creating the Network

With the locations of the ground stations and Starlink satellites determined, we calculated the intersatellite link and links between ground stations and satellites to create the network topology. Starlink satellites will eventually share data with optical intersatellite links, allowing the system to transmit information and carry internet traffic, however the openly available information about these intersatellite links and the corresponding subsystems is sparse. To determine which links were possible in the network, we considered

three network constraints: visibility, range, and hardware limitations. Each constraint is described in detail below:

1. **Range:** The distance between two satellites determines whether they can establish a link.
2. **Visibility:** The visibility between two satellites, which is also referred to as Line-Of-Sight (LOS), indicates if the satellite can receive the transmitted signal from another satellite without reflection or occlusion of the signal. Assuming that the ionosphere occludes signals and is opaque below an altitude of 80 km, simple geometry gives a maximum link length of 5016 km at an altitude of 550 km [2,8,9]
3. **Hardware:** The range and the LOS place physical constraints on potential links, but the design of the satellites themselves also determines how many links are feasible. For example, the number of laser links that each satellite can support is limited by the number of optical heads on each satellite.

To calculate the Cramér-Rao Bound for Starlink, we assumed a network topology in which satellites are connected to two satellites in the same orbital plane and two in neighbouring planes, as described in [9]. This is shown in Figure 3 for the full Starlink network. We also assumed that any Starlink satellite within range of a ground station—as discussed in Section 2.2—was connected to the ground station. The resulting network topology was used in all our calculations of the Cramér-Rao Bound.

2.4 Exploring the Network

In [8], the authors classify and analyse the time-varying links available in the Starlink constellation. The orbital dynamics of LEO constellations means that the number of intersatellite links a single satellite can make varies over the course of an orbit. The results of a similar analysis based on the orbital configuration of Phase 1 of Starlink is shown in Figures 4 and 5. As the figures show, the greatest number of possible connections occur at mid-latitudes. After analysing the time-varying links possible in the Starlink constellation we established that the Starlink satellites can connect to around 40 other satellites under only the physical constraints of visibility.

3. Calculating the Cramér-Rao Bound

In this section we summarise cooperative localisation problems and the CRB before describing our calculations and simulations.

3.1 Cooperative Localisation Problems

The set-up for cooperative localisation problems is described in detail in [15]. In brief, the 3-dimensional cooperative sensor location estimation problem can be stated as follows. Consider n nodes with unknown locations and m anchor nodes with exactly known locations. The problem is to estimate the $3n$ unknown coordinates $\theta = [\theta_x, \theta_y, \theta_z]$, where $\theta_x = [x_1, x_2, \dots, x_n]$, $\theta_y = [y_1, y_2, \dots, y_n]$, $\theta_z = [z_1, z_2, \dots, z_n]$ given the location of the anchor nodes, $[x_{n+1}, \dots, x_m, y_{n+1}, \dots, y_m, z_{n+1}, \dots, z_m]$ and a collection of distance measurements between the nodes.

Treating the $n=1584$ Starlink satellites as the unknown nodes and the $m=87$ ground stations as anchor nodes with known locations and considering the network topology described in Section 2.3 it is possible to frame our model of Starlink as a cooperative localisation problem for a wireless sensor network and thus to calculate the Cramér-Rao Bound.

3.2 The Cramér-Rao Bound

The Cramér-Rao Bound (CRB) provides a lower bound on the variance that can be achieved by any unbiased estimator [16] [17]. The CRB is one of many performance bounds can be used to determine the 'best case' performance of an estimator at a given location with given information and using a given technique.

The bound is affected by several parameters, including:

- The number of sensors with unknown locations (nodes n) and the number of sensors with known locations (anchors m)
- The relative locations of nodes
- Dimensionality (2D or 3D)
- Type of measurement
- Link characteristics
- Network topology

3.3 Calculating the Cramér-Rao Bound

In practice, the CRB can be determined by inverting the Fisher Information Matrix (FIM), denoted \mathbf{F} . Inverting the 3-by-3 FIM gives the CRB matrix whose diagonals are the best achievable x, y , and z position variances. To generate a single figure of merit, we calculated the square Root of the CRB (RCRB) for the x, y , and z position using $(\frac{1}{3} \text{tr}\mathbf{F}^{-1})^{1/2}$, where $\text{tr}\mathbf{F}^{-1}$ is the trace of the inverse FIM. At each timestep in our simulation, an individual Fisher matrix for each satellite was calculated using the location of the satellite and the network topology using equation 2.

$$\mathbf{F} = \gamma \begin{bmatrix} \mathbf{F}_{xx} & \mathbf{F}_{xy} & \mathbf{F}_{xz} \\ \mathbf{F}_{xy}^T & \mathbf{F}_{yy} & \mathbf{F}_{yz} \\ \mathbf{F}_{xz}^T & \mathbf{F}_{yz}^T & \mathbf{F}_{zz} \end{bmatrix} \quad (2)$$

Where each of the entries in \mathbf{F} were calculated from the following equations:

$$\begin{aligned}
 \mathbf{F}_{xx} &= \sum_{j \in H(i)} (x_i - x_j)^2 / d_{ij}^s \\
 \mathbf{F}_{yy} &= \sum_{j \in H(i)} (y_i - y_j)^2 / d_{ij}^s \\
 \mathbf{F}_{zz} &= \sum_{j \in H(i)} (z_i - z_j)^2 / d_{ij}^s \\
 \mathbf{F}_{xy} &= \sum_{j \in H(i)} (x_i - x_j)(y_i - y_j) / d_{ij}^s \\
 \mathbf{F}_{xz} &= \sum_{j \in H(i)} (x_i - x_j)(z_i - z_j) / d_{ij}^s \\
 \mathbf{F}_{yz} &= \sum_{j \in H(i)} (y_i - y_j)(z_i - z_j) / d_{ij}^s
 \end{aligned} \tag{3}$$

where $H(i)$ is the set of nodes with which satellite i can communicate and consists of the four connected satellites as well as any ground stations within range. d_{ij} is the distance between the Starlink satellite i and connected satellite or ground station j with position $[x_j, y_j, z_j]$. s and γ are respectively an exponent and a channel constant dependent on the type of measurement. In our simulations, we assumed Time of Arrival (ToA) measurements with $s=2$ and γ given by:

$$\gamma = \frac{1}{(v_p \sigma_T)^2} \tag{4}$$

where v_p is the propagation velocity of the signal and σ_T is the standard deviation of the ToA measurements. We assumed a value of $\gamma = 29, 860$ in our calculations

3.4 Simulations

We simulated a full orbit of $T=1.59$ hours at 10-second time increments for a total of 573 time steps. At each timestep, we calculated the instantaneous CRB of all Starlink satellites by calculating and inverting the Fisher matrix for all 1584 satellites. To obtain a single figure of merit, we calculated the RCRB for each Starlink satellite at every timestep.

4. Results & Discussion

Our results that the position of Starlink satellites can be determined from intersatellite measurements to an accuracy of approximately $\text{RCRB} = 10.15$ metres for most of their orbit. However, this result is highly dependent on the link characteristics γ assumed when calculating the CRB. Figure 6 shows the variation in RCRB for a single satellite (s01001) over a single orbit, and this variation has a maximum of 36.5 m and a minimum of approximately 2m. These significant peaks

in the RCRB over the orbit occur at high latitudes and indicate sections of the orbit where the satellite's position can be determined less accurately. This occurs because the geometrical arrangement of connections with other satellites is less evenly distributed at high latitudes than during the rest of the orbit. This is similar to dilution of precision in Global Positioning Satellites, where closely aligned satellites results in a lower position accuracy. This effect was visible in our explorations of the Starlink network, and can be seen in Figure 5d, in which the connections to other satellites are more closely aligned. The RCRB for satellite s01001 decreases as the satellite passes over a ground station in southern Chile. The pass of above this ground station is shown in greater detail in Figure 7, which shows the ground track over Tierra del Fuego and the corresponding RCRB. The RCRB drops by around 50% as soon as it is within communication range of the ground station at Puerto Montt. While the RCRB is reduced by the connection to a ground station, the underlying trend in the RCRB is unchanged. This trend is driven by the changing geometry of the Starlink network and can be seen as the gradual decrease in the RCRB even while the satellite is in range of the Puerto Montt ground station.

In general, our results are similar to those reported for other constellations using cooperative intersatellite navigation [2] but also show room for improvement. We discuss avenues for future research and ongoing work in the next section.

5. Conclusions

Our results are comparable to those reported for small constellations using cooperative intersatellite navigation [2] but also show room for improvement; these results are highly dependent on the link characteristics assumed when calculating the RCRB and ignore the dynamics of the system. In future, calculations of performance bounds on cooperative localisation in Starlink could be improved by considering the orbital dynamics of the satellites, for example by combining intersatellite cooperative navigation measurements with an Extended Kalman Filter that considers system dynamics. The results presented here also only consider the anchored case, meaning that our calculations included intersatellite measurements in Starlink as well as measurements from ground stations. We are currently in the process of preparing an extended analysis comparing the anchored CRB results presented here with a simulation of cooperative localisation without input from ground stations.

Acknowledgements

Dr. R.T.Rajan is partially funded partially by the Dutch-PIPP (Partnerships for Space Instruments

Applications Preparatory Programme), funded by NWO (Netherlands Organisation for Scientific Research) and NSO (Netherlands Space Office).

References

- [1] Walker, Constance, et al. Impact of satellite constellations on optical astronomy and recommendations toward mitigations. *Bulletin of the American Astronomical Society* 52.2 (2020).
- [2] Dave, Pratik Kamlesh. Autonomous navigation of distributed spacecraft using intersatellite laser communications, Ph.D. thesis, Massachusetts Institute of Technology (2020).
- [3] X. Li, Z. Jiang, F. Ma, H. Lv, Y. Yuan, X. Li, Leo precise orbit determination with intersatellite links, *Remote Sensing* 11 (18) (2019)
- [4] Starlink webpage (Accessed August 30th 2022) <https://www.starlink.com>
- [5] Boley, Aaron C., and Michael Byers. Satellite megaconstellations create risks in Low Earth Orbit, the atmosphere and on Earth. *Scientific Reports* 11.1 (2021): 1-8.
- [6] Hainaut, Olivier R., and Andrew P. Williams. Impact of satellite constellations on astronomical observations with ESO telescopes in the visible and infrared domains. *Astronomy & Astrophysics* 636 (2020): A121.
- [7] McDowell, Jonathan C. The low earth orbit satellite population and impacts of the SpaceX Starlink constellation. *The Astrophysical Journal Letters* 892.2 (2020): L36.
- [8] Chaudhry, Aizaz U., and Halim Yanikomeroglu. Laser intersatellite links in a starlink constellation: A classification and analysis. *IEEE Vehicular Technology Magazine* 16.2 (2021): 48-56.
- [9] Bhattacharjee, Debopam, and Ankit Singla. Network topology design at 27,000 km/hour. *Proceedings of the 15th International Conference on Emerging Networking Experiments And Technologies*. 2019.
- [10] W. Wiltshire, Application for Fixed Satellite Service by Space Exploration Holdings, LLC (Apr. 2020). Accessible at <https://fcc.report/IBFS/SAT-MOD-20200417-00037>
- [11] C. Turner, R. T. Rajan, Simulated megaconstellation ephemerides (2021). IEEE Datport doi:10.21227/s1qk-xt91. Accessible at <https://dx.doi.org/10.21227/s1qk-xt9>
- [12] C. Turner, Github (2021). Accessible at <https://github.com/CalumTurnerAstro/>
- [13] Rodríguez, Juan Luis Cano, Helge Eichhorn, and Frazer McLean. Poliastro: an astrodynamics library written in python with fortran performance. 6th International Conference on Astrodynamics Tools and Techniques.
- [14] Cakaj, Shkelzen, et al. The Range and Horizon Plane Simulation for Ground Stations of Low Earth Orbiting (LEO) Satellites. *Int. J. Commun. Netw. Syst. Sci.* 4.9 (2011): 585-589.
- [15] Patwari, Neal, et al. Locating the nodes: cooperative localization in wireless sensor networks. *IEEE Signal processing magazine* 22.4 (2005): 54-69.
- [16] Kay, Steven M. *Fundamentals of statistical signal processing: estimation theory*. Prentice-Hall, Inc., 1993.
- [17] Van Trees, Harry L. *Detection, estimation, and modulation theory, part I: detection, estimation, and linear modulation theory*. John Wiley & Sons, 2004.
- [18] Cakaj, Shkelzen. "The Parameters Comparison of the "Starlink" LEO Satellites Constellation for Different Orbital Shells." *Frontiers in Communications and Networks* 2 (2021): 643095.

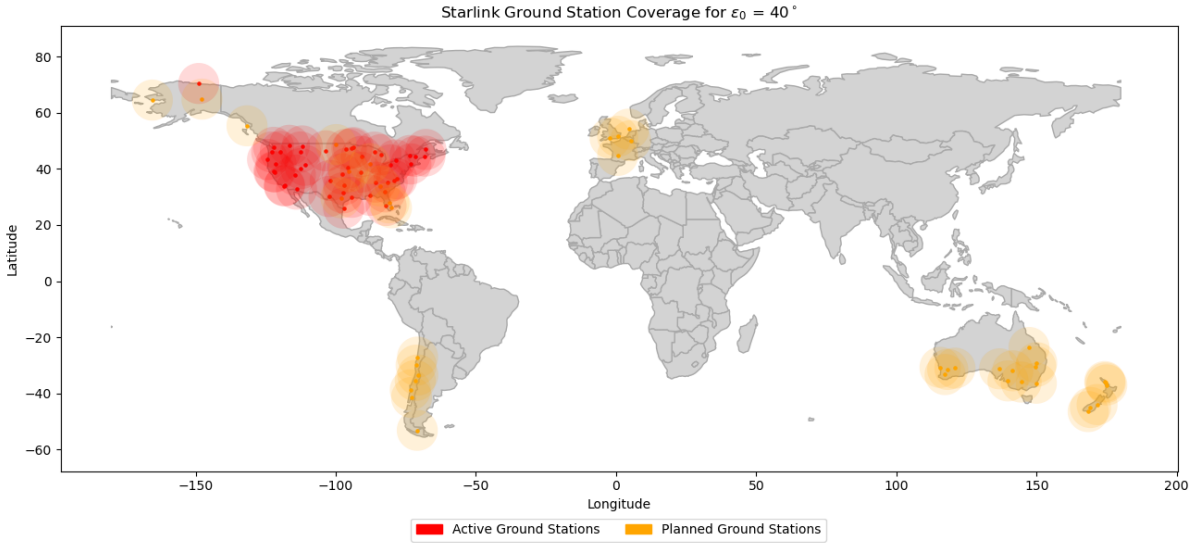


Fig. 1. The locations of 87 planned and active Starlink ground station and their coverage assuming $\epsilon_0 = 40^\circ$ [18]. The locations of the ground stations are substantiated by regulatory filings in the USA, Chile, France, the UK, Australia, and New Zealand. All latitudes and longitudes are approximate and correct at the town/city level. A value of $\epsilon_0 = 40^\circ$ gives a visibility range of $d = 812$ km.

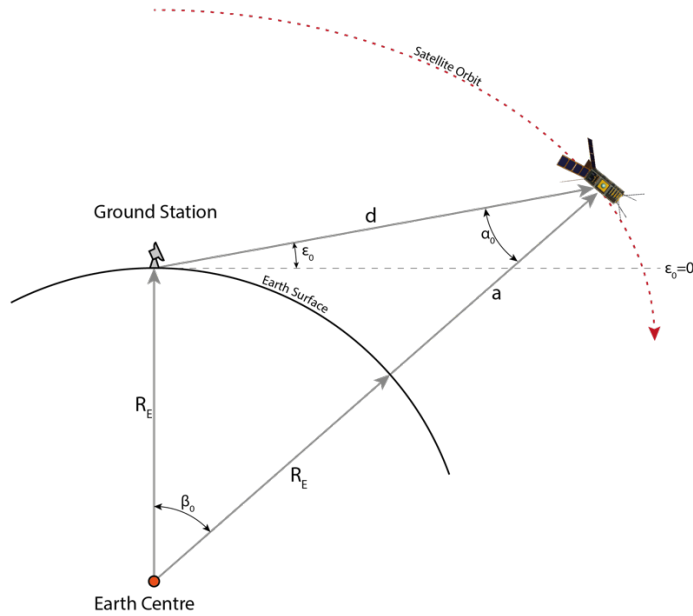


Fig. 2. A diagram of the geometric set-up used to calculate the visibility of satellites from a ground station. The satellite has an altitude of a and makes an angle of ϵ_0 with the ground station's local horizon. The maximum distance at which the satellite is visible from the ground station considering only line of sight can be found by determining d . Diagram adapted from [14]

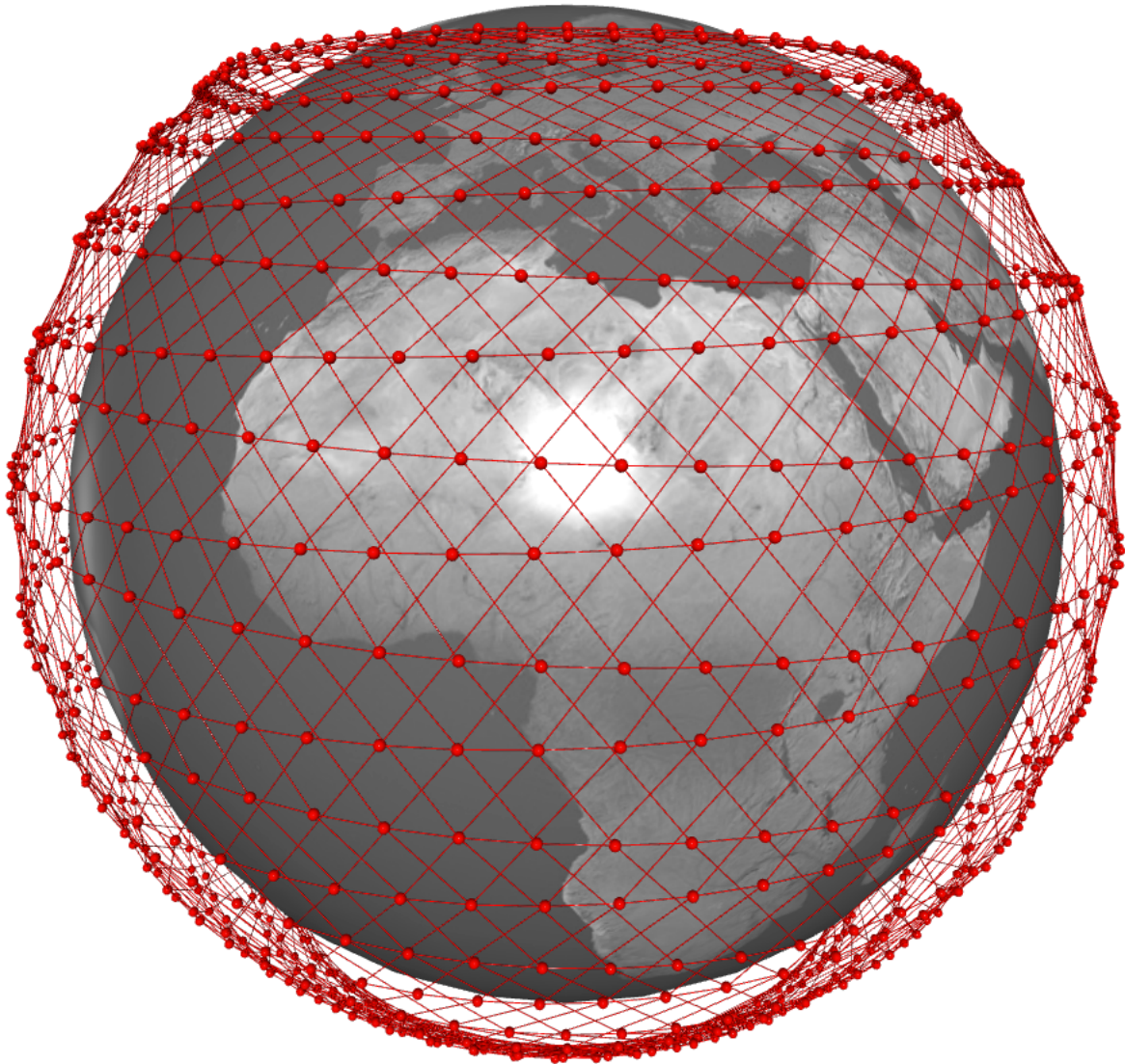


Fig. 3. Full network of the Starlink mega-constellation assuming a network topology in which satellites are connected to two satellites in the same orbital plane and two in neighbouring planes. The 1584 satellites are distributed evenly across 72 orbital planes with 22 satellites in each plane.

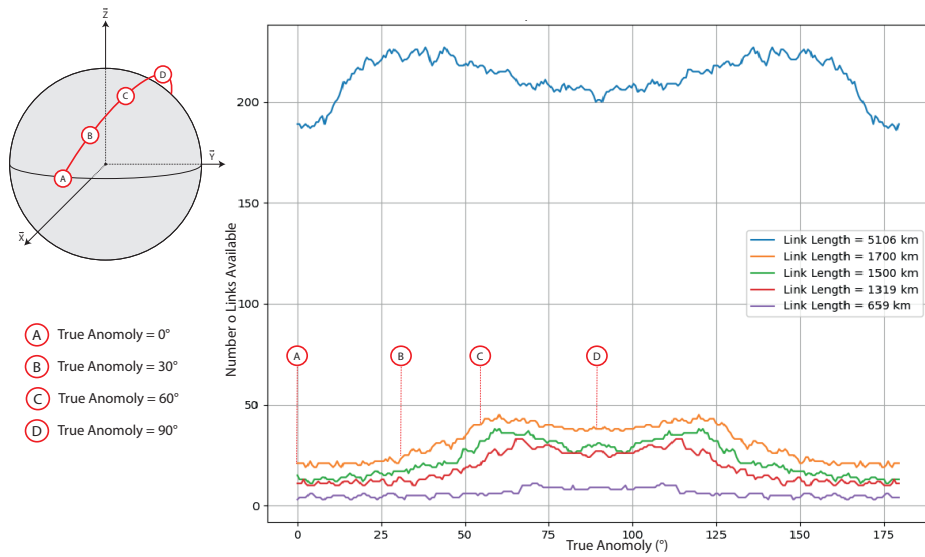


Fig. 4. Graph of the number of possible links against true anomaly for swarm agent s01001 with a variety of maximum link lengths from 659 km to 5016 km. The snapshots A-D are rendered in Figure 4.6. The orbital dynamics of Starlink mean that the number of possible connections is highly time-varying. As the graph shows, the greatest number of possible connections occurs at mid-latitudes of roughly 60°, and unsurprisingly a greater maximum link length results in a greater number of possible connections.

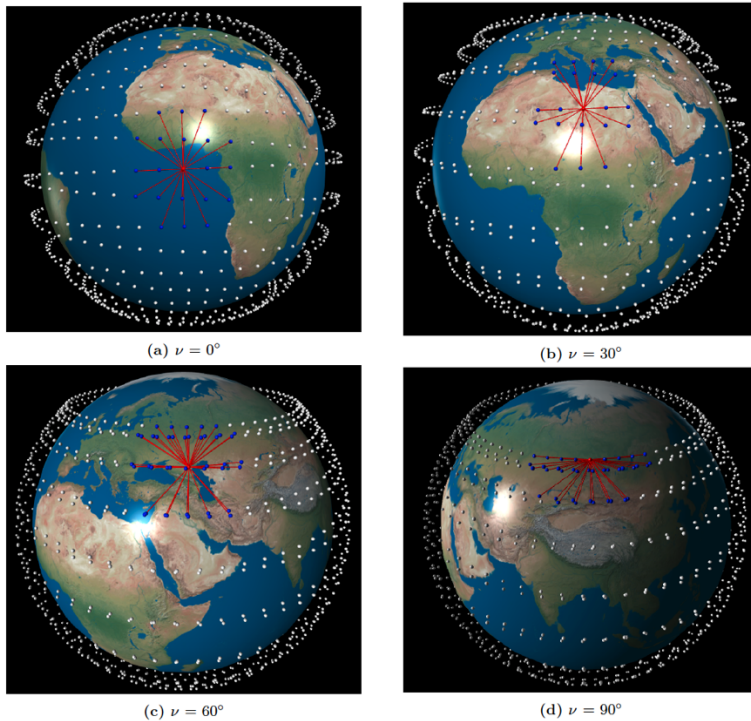


Fig. 5. Possible connections in the Starlink network highlighted at different points in the orbit for a maximum link length of 1700 km. A graph of the time-varying number of links at each point is shown in Figure 4. The snapshots are identified by the true anomaly, ν , of the satellite shown red, swarm agent s01001. Connected satellites are shown in blue. The figure demonstrates the same result as Figure 4.5, namely that the number of possible links in Starlink Phase 1 is greatest at latitudes of roughly 60° and least above the equator.

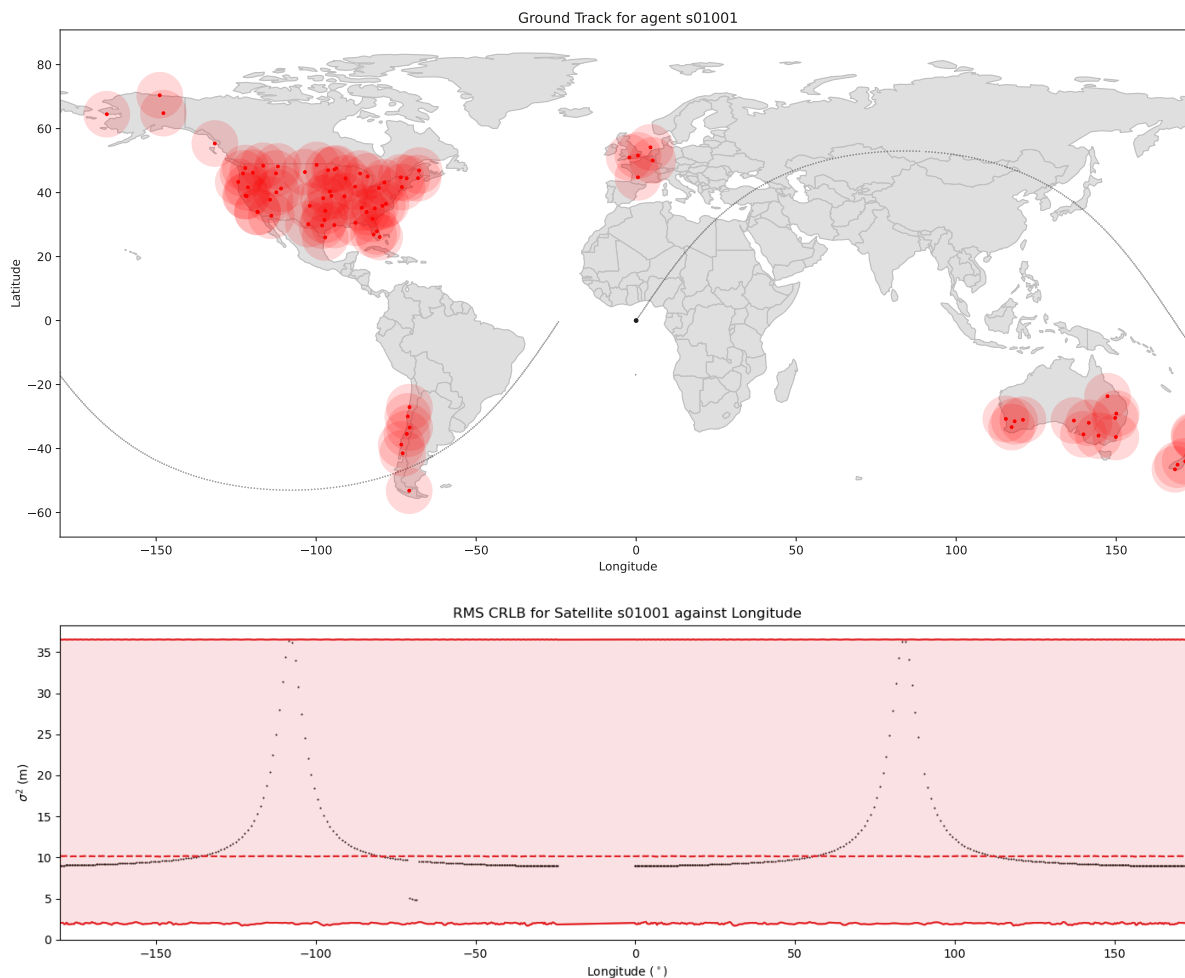


Fig. 6. The upper figure shows the ground track for satellite s01001 as well as the position of the Starlink ground stations. The lower figure shows the RCRB (here denoted σ^2) against longitude, with the average RCRB for the constellation shown as a dashed red line and the area between the maximum and minimum values for the constellation shaded in red. Referring to the two plots, it is clear that the peaks in the RCRB correspond to the highest and lowest latitudes for s01001's orbit, and that the trough in the RCRB occurs when s01001 is in range of a ground station in South America. The pass of s01001 over the ground station is shown in detail in Figure 7.

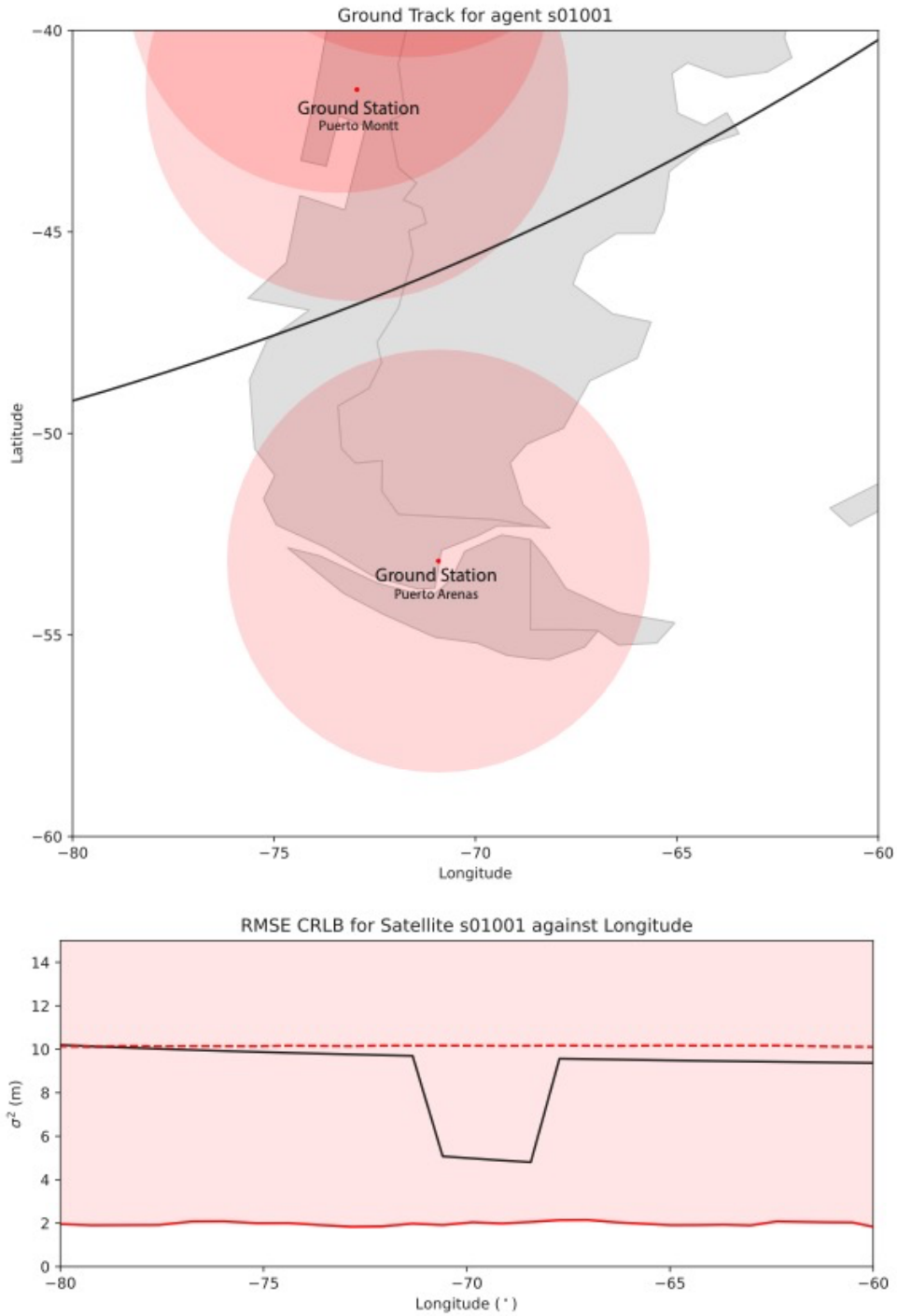


Fig. 7. The figure shows satellite s01001 passing over Tierra del Fuego at the southernmost tip of Chile, as well as the RCRB during this pass (here denoted σ^2). Comparison of the two plots shows that the RCRB drops by roughly 50% while it is in range of the ground station at Puerto Montt. The overall trend in the RCRB, which is a gradual decrease driven by the geometry of the Starlink network, continues even while s01011 is in range of the ground station.